Transfer of Load Between Precast Bridge Slabs

ADRIAN PAUW and JOHN E. BREEN, respectively, Professor and Assistant Professor of Civil Engineering, University of Missouri, Columbia

● THIS PAPER presents the procedures used and the results obtained in a series of static load tests designed to study the mechanism of load transfer between adjacent precast bridge-slab sections. These tests were undertaken as one phase of a general structural and economic study of precast bridge units under the sponsorship of the Missouri State Highway Commission and the Bureau of Public Roads. Because little or no information was available on the nature of the mechanism of load transfer between precast slab sections, this test program was necessarily of an exploratory nature and was therefore designed to give specific information for the standard channel sections presently used by the Missouri State Highway Department.

THE MISSOURI STANDARD CHANNEL SECTION

The precast channel section used by the Missouri State Highway Department has a standard width of 3 ft 2 in., and a depth of 18 in. Sections of the same depth may be used for either H-10 or H-15 loading by providing different amounts of longitudinal reinforcement. The standard lengths range from 21.5 to 34 ft in modular increments of 6.25 ft. Typical details are shown in Figure 1. Seven parallel units are used for a 20-ft roadway and an additional special 2-ft wide unit, for a 22-ft roadway. Stiffening diaphragms are provided at 6 ft 3 in. on centers and the units are bolted together at points midway between the diaphragms using 1-in.-diameter bolts with beveled washers at each end.

Three holes are provided in the channel legs at each bolt location to permit use of the units in skewed structures. The design provides for shear transfer between units by the 1-in.-diameter tie bolts and by a $\frac{3}{4}$-in.-wide keyway filled with a dry-packed cement mortar to within 1 in. of the top surface. After the units are erected an asphalt wearing surface is placed to provide a smooth riding surface.

DETAILS OF TEST ARRANGEMENT

The sections were too large to permit full-scale testing for all length and load combinations. In the static-load test program for the individual units, half-scale models were therefore selected to simplify handling. The results of the model tests were correlated by one set of full-scale tests, using the 21.5-ft span. The results obtained from tests of the half-scale model were found to be in excellent agreement with test results for the full-size sections. Similarly full-scale testing for the load transfer series was not feasible because of laboratory space limitations and it was therefore decided to limit the test to a study of the behavior of three half-scale models of the standard 27.75-ft section for H-10 loading. Dimensions of the model section are also shown in Figure 1.

The shear keys provided in the model section were scaled down to be representative of the keys used in the prototype. Figure 2 shows an over-all view of the test frame and the test arrangement. Load cells were provided at the reaction points under each channel leg and the load was applied through a calibrated load cell by means of a hydraulic jack. Other instrumentation was provided to measure deflections, slip between units, and strains in the reinforcement and in the concrete.

To separate the effect of the tie bolts from that of the shear keys, the units were loaded in a preliminary series of tests in which shear transfer was provided by the tie bolts alone. Care was taken in this series not to overload the units and thereby damage the sections before the final tests. On completion of this test series the tie bolts were

loosened and the keys packed with a dry cement-mortar grout consisting of one part portland cement and two parts sand. The tie bolts were then retightened. A close-up of the key detail is shown in Figure 3.

TESTING PROGRAM

To permit comparison with the test results for the individual sections the three half-scale model sections used in the load transfer series were made as nearly identical as possible with the sections used in the flexural capacity series. To obtain the maximum amount of information possible with a single set of specimens, a special loading sequence was followed. This sequence can best be explained by referring to Figure 4.

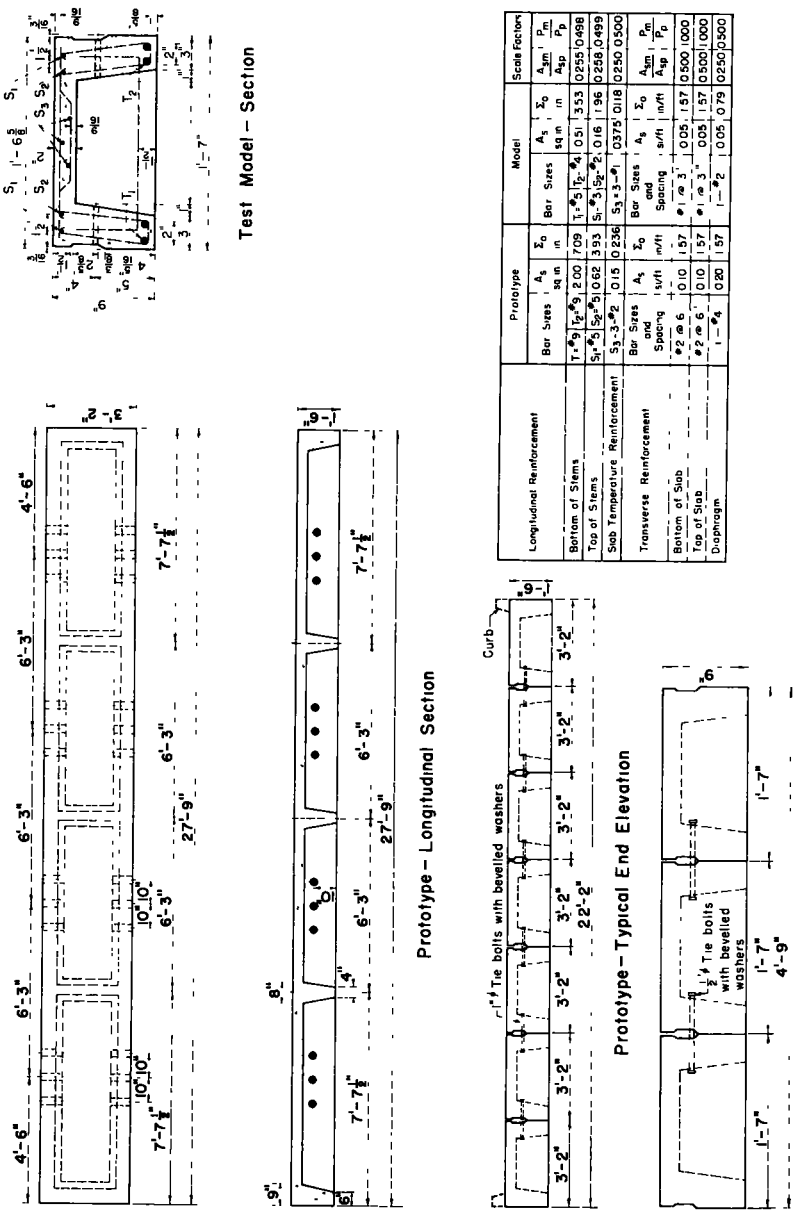

Longitudinal Reinforcement	Prototype				Model				Scale Factors	
	Bar Sizes	A_s sq in	Σ_0 in		Bar Sizes	A_s sq in	Σ_0 in		$\frac{A_{sm}}{A_{sp}}$	$\frac{P_m}{P_p}$
Bottom of Stems	T_1-#9, T_2-#9	2.00	.709		T_1-#5, T_2-#4	.051	.353		.0255	.0498
Top of Stems	S_1-#5, S_2-#5	.062	.393		S_1-#3, S_2-#2	.016	.196		.0258	.0499
Slab Temperature Reinforcement	S_3-3-#2	.015	.0236		S_3-3-#1	.0375	.0118		.0250	.0500
Transverse Reinforcement	Bar Sizes and Spacing	A_s sq in/ft	Σ_0 in/ft		Bar Sizes and Spacing	A_s sq in/ft	Σ_0 in/ft		$\frac{A_{sm}}{A_{sp}}$	$\frac{P_m}{P_p}$
Bottom of Slab	#2 @ 6	.010	.157		#1 @ 3	.005	.157		.0500	.1000
Top of Slab	#2 @ 6	.010	.157		#1 @ 3	.005	.157		.0500	.1000
Diaphragm	1 – #4	.020	.157		1 – #2	.005	.079		.0250	.0500

Figure 1. Details of standard channel test sections.

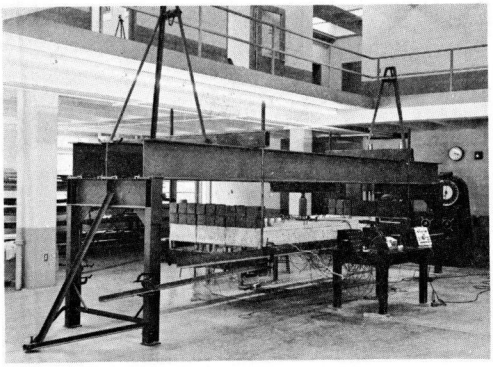

Figure 2. Test arrangement.

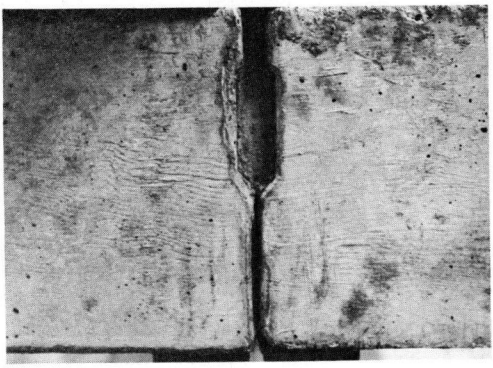

Figure 3. Closeup of key detail.

Seven methods of load application were used. In series I, II, and III, the load was applied at the midpoint of the center, the west, and the east channel, respectively. In series IV and V the load was applied at the north quarter-point of the center and of the west channel, respectively. Finally, in series VI and VII the load was split and applied to the outside channels at the center, and at the north quarter-point, respectively.

The test series with the joints grouted were designated by subscripts, where the subscript letter defined the maximum load applied in the particular series. While this loading sequence permitted obtaining the maximum amount of information, it did complicate interpretation of the measurements, especially for the load ranges for which the loading sequence resulted in cumulative increments of permanent distortion. The sequence of loading, showing the loading limits, is summarized in Table 1.

INSTRUMENTATION

The disposition of the instrumentation used in the test is shown in Figure 5. The instruments used and their points of application were as follows:

1. One pancake-type load cell, 60,000-lb capacity, used to measure the applied load.
2. Twelve spool-type load cells, 10,000-lb capacity, under the channel stems to measure the reactions.
3. Twelve deflectometers, one 1.0-in. range deflectometer under each channel stem at the center of the span, and one 0.5-in. range deflectometer at the center of the diaphragm at the one-quarter and at the three-quarter points of each channel.
4. Eighteen SR-4 strain gages to measure the longitudinal steel strains in each stem; six each, at the one-quarter, the center, and the three-quarter points.
5. Six SR-4 strain gages to measure the transverse stell strains in the diaphragms of the center and west channels at the one-quarter, the center, and the three-quarter points.
6. Nine extensometers to measure the concrete strains in each of the interior diaphragms.
7. Six extensometers mounted directly above the center of each stem, to measure the concrete strains at the center of the span.
8. Two pairs of slip gages, mounted between channels at the center of the span, to measure slip and rotation of the channel sections.
9. Twelve bench marks for auxiliary large deflection measurements with a height gage.

Figure 6 shows a bank of reaction cells in place. The precast sections were carefully grouted on the reaction-cell bearing plates, to equalize the initial dead-load reactions. Some difficulty was encountered with the use of these cells in that their accuracy at very low loads was impaired by mechanical hysteresis and zero drift.

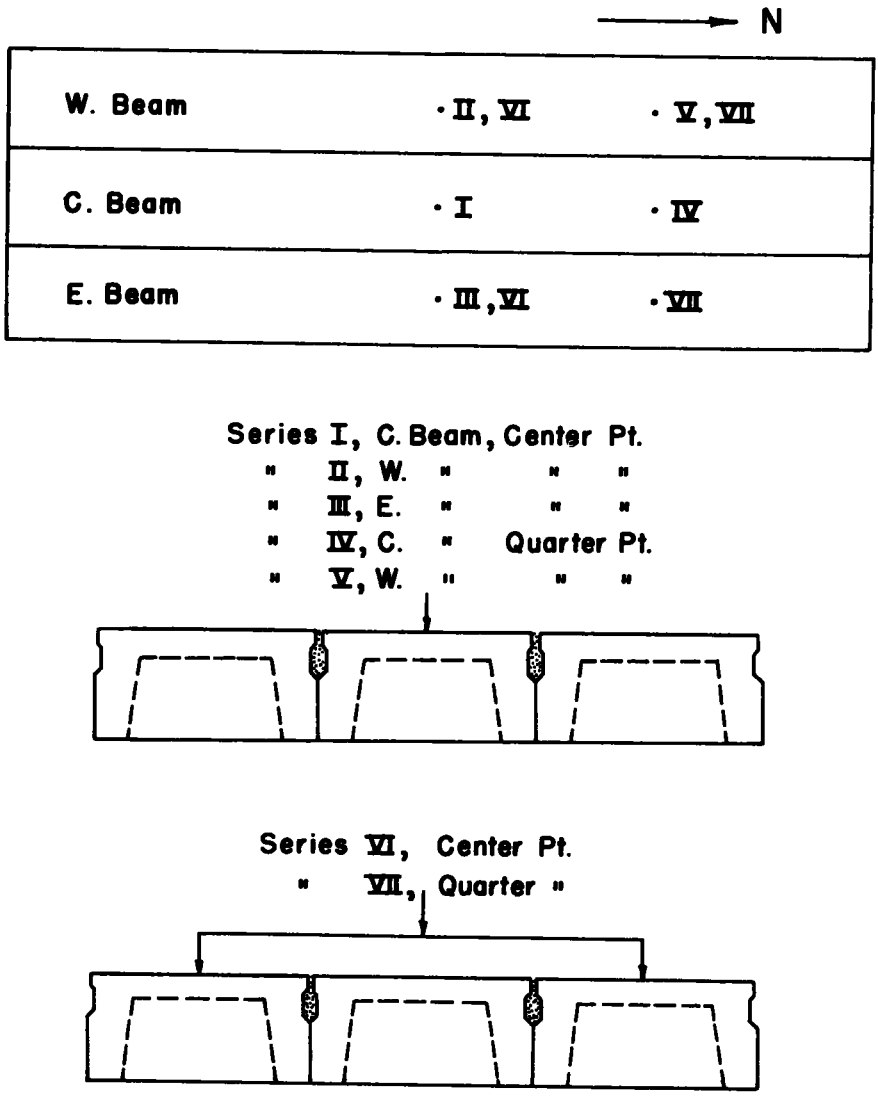

Figure 4. Loading sequence.

This difficulty was overcome by preloading the cells by placing six 50-lb weights on the end of each section.

The plunger-type deflectometers used are shown in Figure 7. These deflectometers were used in place of dial gages because of the inaccessibility of the deflection stations and because their use permitted measurements to be made from a central location. The deflectometers were supported by a steel framework resting on the reaction supports of the testing frame as shown in Figure 6. When the deflections became large, the deflectometers were removed and deflections measured with the height gage shown in Figure 8 using tensioned wires attached to the testing frame as reference base lines. The height gage was provided when a vibrating reed the vibration of which was damped when the reed came in contact with the base-line wire thus giving a sensitive

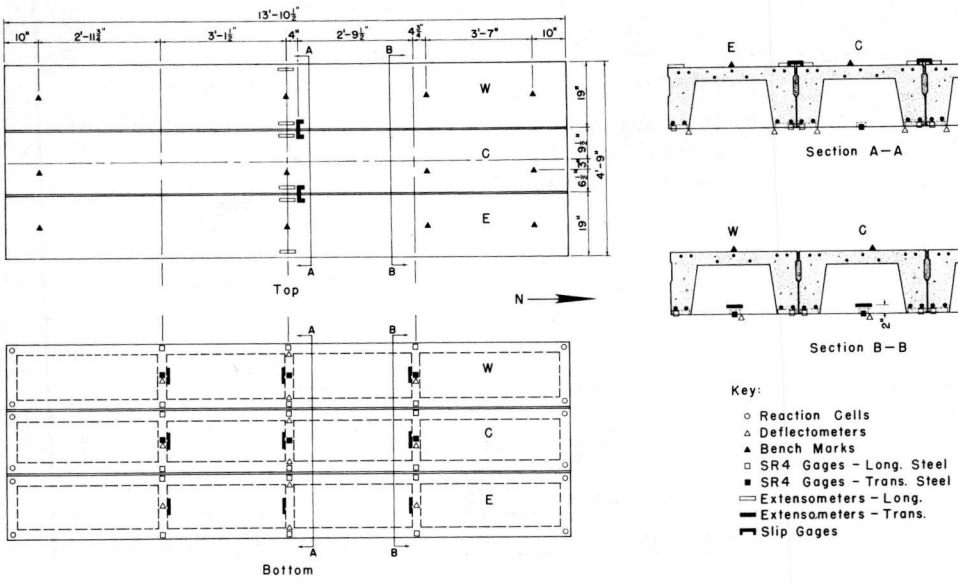

Figure 5. Instrumentation.

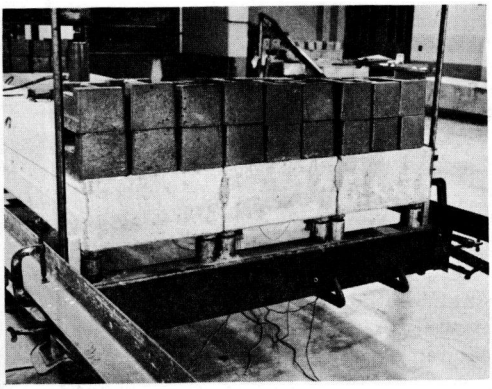

Figure 6. Bank of reaction cells.

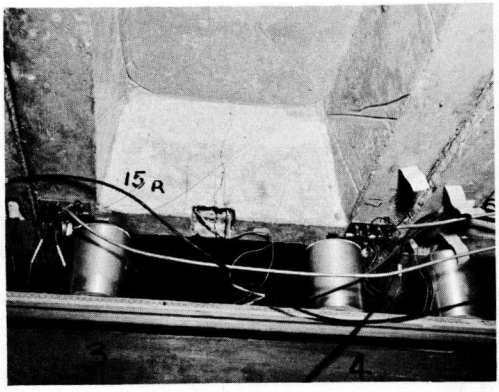

Figure 7. Deflectometers.

indication of position. The micrometer adjustment on the height gage permitted the determination of deflections to an accuracy of about 0.002 in.

Figure 7 also shows the areas of concrete blocked out to permit attachment of SR-4 gages. Reinforcement was prepared for gage installation before casting the channels and small sections of concrete were blocked out with pieces of styrofoam. After hardening of the concrete, the pieces of styrofoam were easily removed and the gages installed. By this technique the need for waterproofing the gages was avoided and all gages were found to operate satisfactorily.

Figure 9 is a close-up view of the clip-on type extensometer used to measure concrete strains. The extensometer (a detailed description of this instrument as well as of the deflectometer and the load cell is given in "Technical Report No. 1, Structural and Economic Study of Precast Bridge Units - Instrumentation," University of Missouri Engineering Experiment Station, 1957) is essentially a three-hinged arch with two SR-4 gages on the center hinge acting as the strain transducer. Inasmuch as two gages are used, one in tension and one in compression, the meter is automatically

TABLE 1A

LOADING

Subletter	Method of Connection	Maximum Applied Load, lb
None	Lateral bolts only	3750
a	Lateral bolts and grouted shear key	3750
b	"	7500
c	"	11250
d	"	15000
e	"	18000
f	"	25000
g	"	30000
h	"	Complete failure

TABLE 1B

LOADING SEQUENCE

Series	Bolts Only	Bolts and Grouted Key							
		a	b	c	d	e	f	g	h
I	1	6	13	20	27	30	31	32	33
II	2	7	14	21	28				34
III	3	8	15	22					35
IV	4	9	16	23					
V	5	10	17	24					
VI		11	18	25	29				
VII		12	19	26					

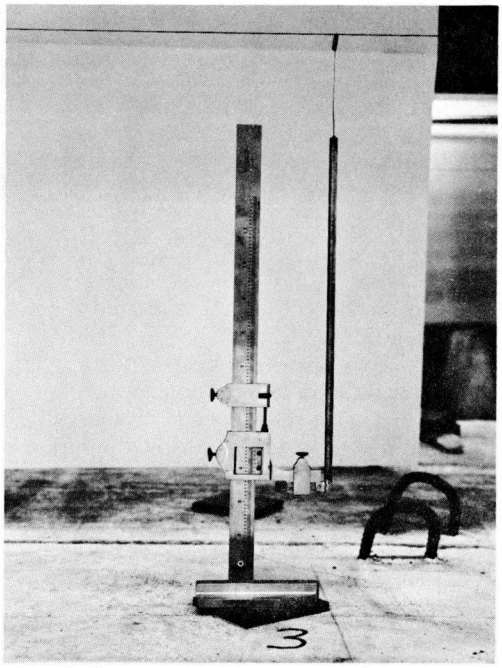

Figure 8. Height gage.

temperature-compensated. A pretensioning screw is provided to permit zero adjustment and to allow application of pretension when the meter is used to measure compressive strains. The meter has a gage length of 4 in. and is attached by cementing the binding posts to the concrete. Figure 10 shows the

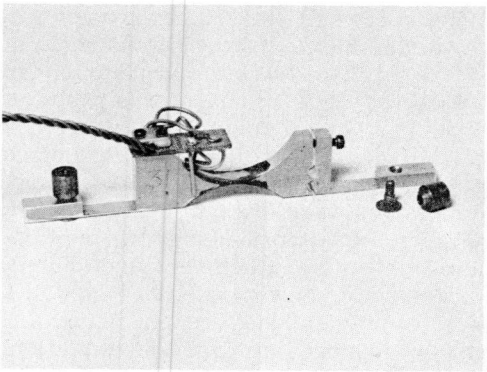

Figure 9. Extensometer.

extensometers installed on the three channel sections. Also shown in this figure are two slip gages and the pancake-type load cell directly under the loading jack.

The details of the slip gage are shown in Figure 11. These gages were patterned after similar instruments used at Lehigh University and were found to perform quite satisfactorily. Both slip and rotation can be determined from the dial readings; relative slip being determined from the difference of the dial increments, and relative rotation, from the sum.

TEST OBJECTIVES

Before discussing the actual test results it is desirable to consider precisely what is to be determined. A single channel unit can carry at most one line of wheel loads acting along the longitudinal centerline of the section. After the units have been joined together by tie bolts and grouted keyways to form an integral bridge slab it is reasonable to expect that part of the load applied to a particular unit will be transferred through shear to the adjacent sections. It is required then to obtain a load transfer coefficient by which the wheel loads may be multiplied to give the effective equivalent design load for a single unit. The present design policy of the Missouri State Highway Department is to consider that the precast units act as a solid slab. The load distribution is then computed by the formula (AASHO, Standard Specifications for Highway Bridges, 7th Edition, p. 25)

$$E = \frac{10N + W}{4N}$$

in which

E = width of slab over which a wheel load is distributed,
N = number of lanes of traffic on the bridge,
W = width of roadway between curbs of the bridge.

Thus for a 20-ft roadway, E = 5 ft giving a load reduction coefficient of 0.63 for a 3-ft 2-in. wide channel section.

The purpose of the load transfer tests, therefore, was to determine load reduction coefficients which can safely be applied in the design of the individual sections. In interpreting the test results for selection of suitable load reduction coefficients the applicability of the tests to actual conditions should be considered carefully. Applicability of any particular test series depends on such factors as (a) the position of the section in the bridge (that is, whether the section is an interior or an edge unit); (b) the length-to-width ratio of the section; and (c) the location of the load.

Some other considerations in selecting a suitable reduction coefficient include (a)

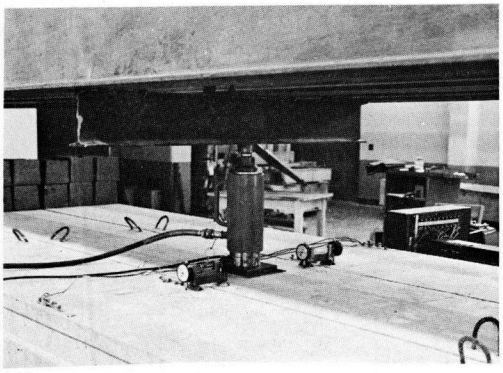

Figure 10. Instrumentation details.

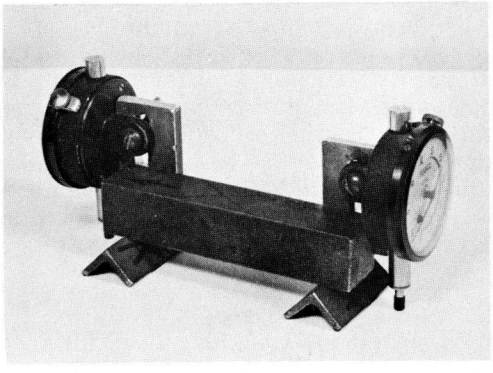

Figure 11. Slip gage.

economic design factors such as the need for interchangeability of precast sections, (b) spacing of the stiffening diaphragms, and (c) the basic design philosophy used (that is, whether the design is to be based on working load stresses or on ultimate load capacity).

The test program completed was not sufficiently extensive to answer all the questions raised by the foregoing considerations. The limited results obtained, however, do indicate very definite behavior patterns and suggest design concepts which should prove useful in planning more extensive investigations.

LIMITATIONS OF MODEL STUDIES

In using structural models it is generally impracticable to preserve a constant model ratio for the effect of both dead and live loads. Because failure of both the single channel sections and of the joined units was primarily due to flexure, the equivalent applied loads used in interpreting the test results were based on equivalent moments; that is, the moments in the model which would result in the same maximum stress levels in the steel and in the concrete in both model and prototype. Thus the equivalent single concentrated load for one line of wheels applied at the midspan of the model was found to be about 3,500 lb based on DL + LL + I for H-10 loading. For two or more working loads the equivalent applied load would have to be increased by increments of 4,100 lb to correct for the dead load of the slab.

SLIP TESTS

The observed maximum slip values in the Series I tests (tie bolts only) are compared with the values obtained in the Series Ia tests (tie bolts and grouted keyways) in Figure 12. Two significant results should be noted:

1. The magnitude of the slip in the Series I tests at an equivalent maximum normal working load was about two-thirds the deflection of a single unit at the same load (see also Fig. 16).
2. The grouting of the keyway reduced the slip in the Series Ia-Ig tests to insignificance. This reduction was further evidenced by the fact that the slip with grouted keyways at ultimate load was considerably less than the slip with tie bolts alone at working load.

From the first result it may be concluded that, although some load transfer may be developed by tie bolts alone at low stress levels, even at normal maximum working load the load transfer ratio has been reduced to insignificance. Furthermore, the relatively large slips at normal working load would tend to cause rapid deterioration of the bituminous wearing surface. On the other hand the grouted keyways were extremely effective in preventing excessive slip up to the ultimate load capacity of the combined sections. The important role of the tie bolts in developing the shearing resistance of the keys should be noted. Their principal function is to prevent lateral separation or spreading of the precast sections and their effectiveness in this respect was demonstrated by the development of stress in the stiffening diaphragms as discussed in a subsequent section.

Figure 13 shows the observed slip values for Series Ia-Ig. The test results have been plotted for the successive load increments of this series so as to give slip as a continuous function of load. The apparent discontinuities are the result of permanent slip displacement due to the cyclic load application used in the tests and the interspacing of the Series II to VI loadings. In spite of these discrepancies it may be noted that the maximum slip just before complete failure of the sections was only about one-third the slip value at working load when tie bolts alone were used.

REACTIONS

The maximum reaction values for each of the Series Ia-Ig tests are shown in Figure The end reactions were averaged for each channel stem. It is of interest that the corner reactions reached a maximum absolute value and then actually decreased as

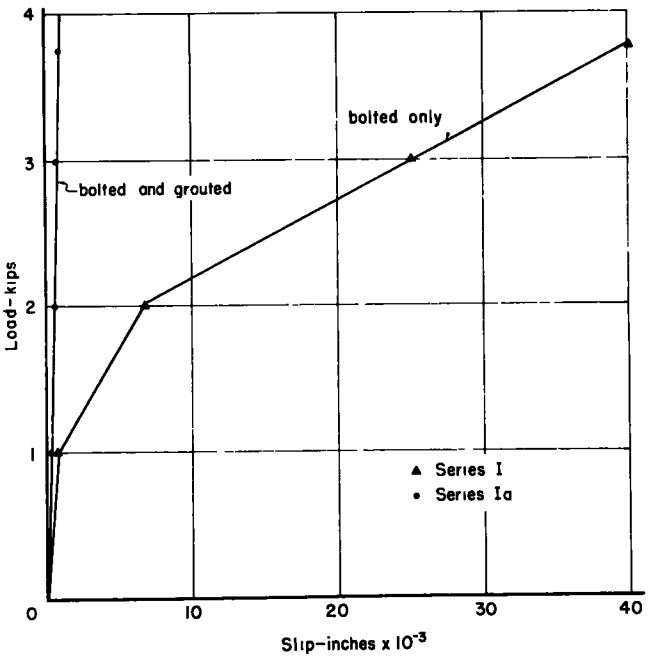

Figure 12. Relative slip.

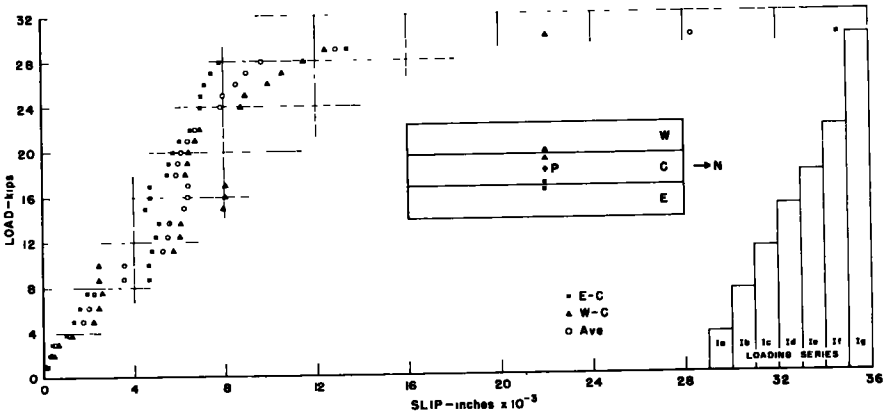

Figure 13. Slip observations—series Ia-Iq.

additional load increments were applied. This phenomenon can be explained by consideration of the redistributuion of the load which resulted from a relatively early yielding of the reinforcement in the stiffening diaphragm of the center channel (see also Fig. 20). This redistribution of load was accompanied by a marked tilting of the exterior channel sections resulting in a sharp increase in the reactions for the interior stems of these sections. These results are perhaps even more graphically demonstrated by Figure 15. Here the reactions are shown as a percentage of the total load applied. It may be noted that the center channel reactions remain relatively constant at a value of about 37 percent of the total load whereas the percentage of the load transmitted to the exterior stems of the unloaded channels decreases and that for the interior stems increases with each additional load increment. While these results cannot be used directly

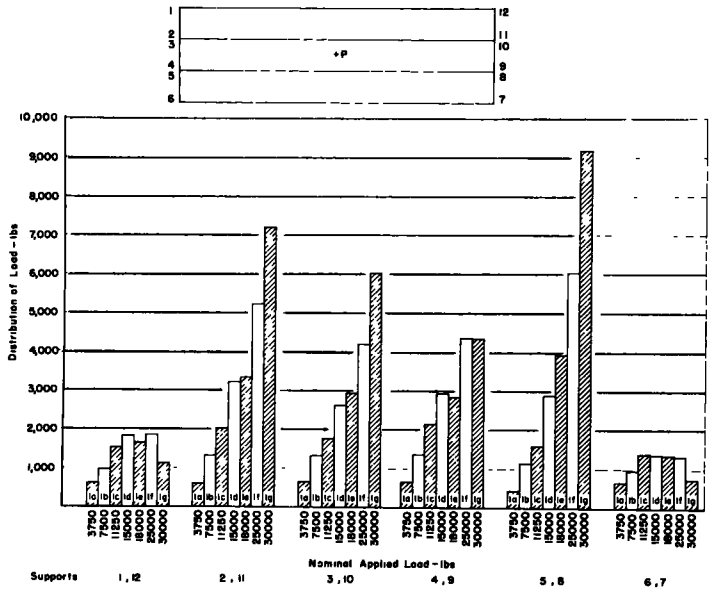

Figure 14. Reactions—series Ia-Ig.

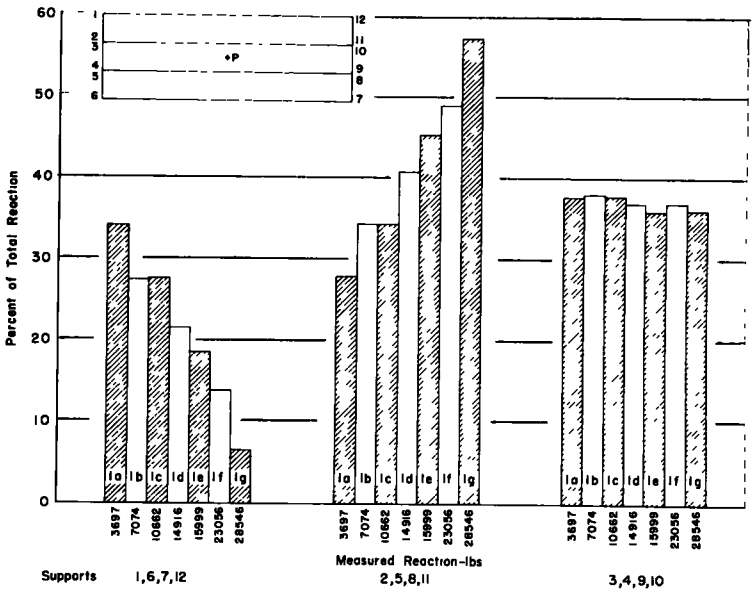

Figure 15. Reaction distribution.

to determine load reduction coefficients, they are useful in obtaining a better understanding of composite action and in providing a measure of the shear distribution between adjoining sections.

DEFLECTIONS

In addition to being an important design criterion in itself, the deflection serves as

an excellent indicator of the strain distribution. Figure 16 compares the center deflections for the connected units with the deflections for a single channel section. With tie bolts alone the deflections of the loaded channel were not significantly reduced, whereas with the keyways grouted and in the elastic range the deflections of the center unit were reduced to about one-third that for a single section.

It may be noted that for the single channel section there was a significant change in slope in the load-deflection curve at an applied load of about 11 kips. This change in slope was caused by yielding of the longitudinal reinforcement. As a result the load-deflection curve is similar in appearance to a typical stress-strain curve for the reinforcement, with the exception that the deflection curve does not become horizontal at the point of initial yield. Following initial yield of the longitudinal reinforcement, the single channel sections were able to sustain some additional load due to shifting of the neutral axis and stressing of the steel into the strain-hardening region.

The change in slope of the load-deflection curve in Figure 16 for the connected units (series Ia-Ig) is more gradual because the main reinforcement did not yield simultaneously in all units resulting in a load redistribution. The deflection of the connected units at failure was only a little over one-third the maximum deflection for the single units because failure was the result of punching of the slab rather than complete collapse of the entire section.

In Figure 17 the deflections of the channel stems at midspan are shown as a percentage of the loaded channel deflection. This figure clearly illustrates the non-linear increase in the tilting of the outside channels as additional load increments were applied. As the ultimate load was approached, the deflections of the outside stems decreased to about 70 percent. The decrease in deflection of the interior stems of the outside channels was in part due to relative slip between the sections. As a consequence of the tilting of the outside channel sections, the longitudinal steel in the adjoining stems started to yield before the yield point of the steel in the outside stem was reached. This initial yielding occurred at about twice the yield load for the single channel section and was followed by a redistribution of the load. At the load level for which the steel strains in the outside stems have reached the yield point, the load-deflection curve (Fig. 16) becomes essentially flat.

Where deflections are the limiting factor in design of relatively shallow slab sections, the load ratio for equivalent deflection at the first yield of the single section would be applicable as a basis for establishing a load reduction coefficient. From Figure 16 it may be seen that for the conditions represented by this test the coefficient would be approximately 11/26 or 0.42. This ratio was found to be consistent with observed strain patterns, because large yields of the longitudinal steel in the outside stems occurred after initial load redistribution and at a load of approximately 26 kips.

LONGITUDINAL STEEL STRAINS

The mechanism of load redistribution due to yielding of the reinforcement is further clairified by the load-strain curves shown in Figure 18. It may be noted that the steel in the center unit yielded at an applied load of about 22 kips followed by yielding of the steel in the interior stems of the outside units at about 25 kips and in the outside stems at 26 kips. The consistent behavior of the reinforcement in corresponding stems should also be noted. A comparison of the initial slopes of these strain curves provides an excellent measure of the load distribution for loads less than the load causing initial yield of the reinforcement in the center channel. Using average slope values the load reduction coefficient determined on this basis was found to be 0.41 for the mid-section.

Unfortunately, no actual data of the steel strains in the vicinity of the yield load were obtained in the tests of the corresponding individual sections, and the comparative strains shown in Figure 19 are therefore based on the known stress-strain characteristics of the reinforcement used in the tests. However the yield load of 11 kips determined on this basis is consistent with the value determined from the load-deflection curve shown in Figure 16. Using these values the load reduction coefficient at yield, following load redistribution, would be 11/26 or 0.42. This value is in excellent agreement with the reduction coefficient determined from the slopes of the strain curves in Figure

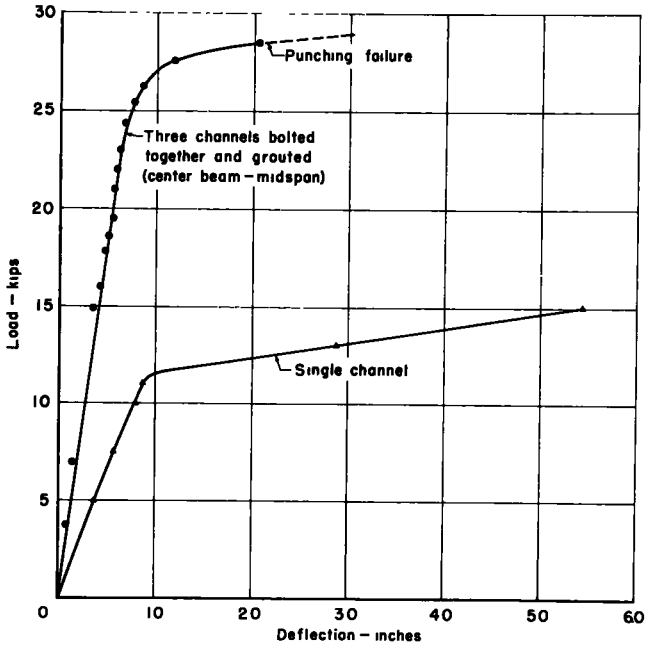

Figure 16. Comparison of channel deflections.

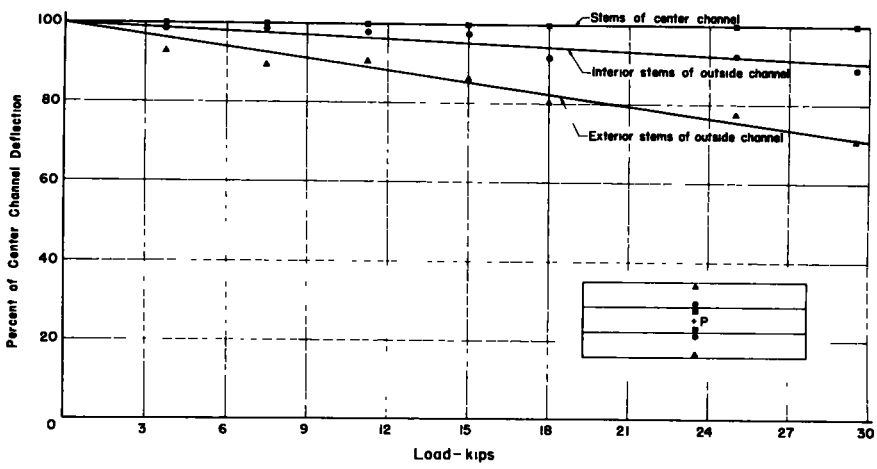

Figure 17. Relative deflection of channel stems.

18. The load reduction coefficient based on behavior at working-stress levels for this case may also be determined by comparing the average slope for the elastic range of the load-strain curves for the center channel with the slope for the single channel. The reduction coefficient determined on this basis is approximately 0.38 for this loading series.

The similarity shown in Figure 18 between the strain curves for the reinforcement in the adjoining channel stems should be noted. While the strains for the stems of the outside channels were somewhat smaller due to rotation and slip, these strains became more nearly equal as the load was distributed. It was also noted that the crack patterns developed in the adjoining stems at these loads were very similar, furth testifying to the effectiveness of the shear keys in distributing the load.

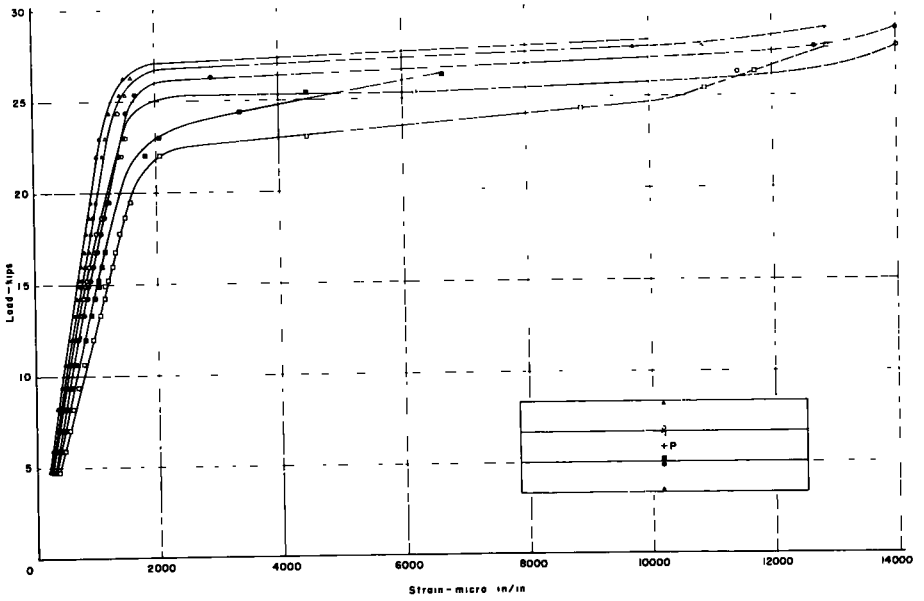

Figure 18. Longitudinal steel strains—series Ia-Ig.

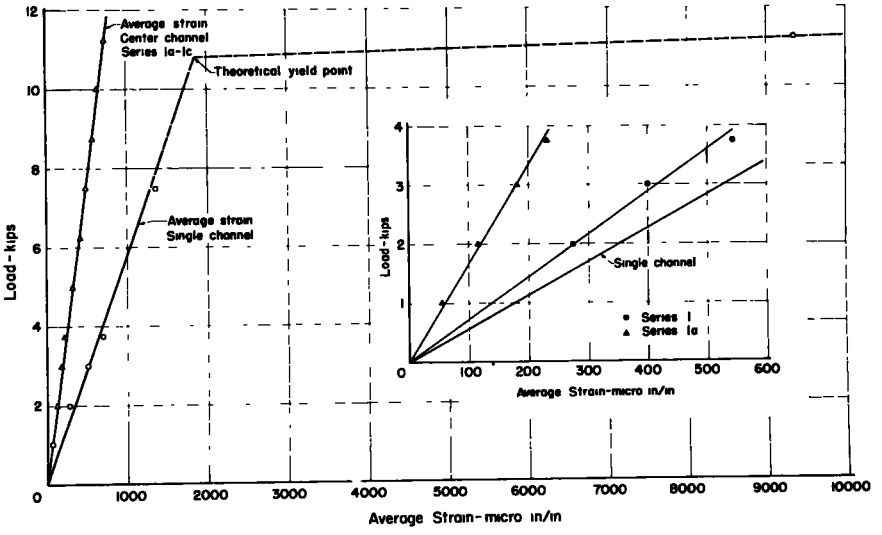

Figure 19. Comparative longitudinal steel strains.

The longitudinal steel strains for the series I test (tie bolts only) are shown in the insert in Figure 19. This plot again confirms the relative ineffectiveness of the use of tie bolts alone in distributing the load.

CONCRETE COMPRESSION STRAINS

The observed strains in the top fibers of the slab above each channel stem are plotted in Figure 20 as a function of applied load. The redistribution of the load to the outside sections is again apparent. The change in slope of the load-strain curves for

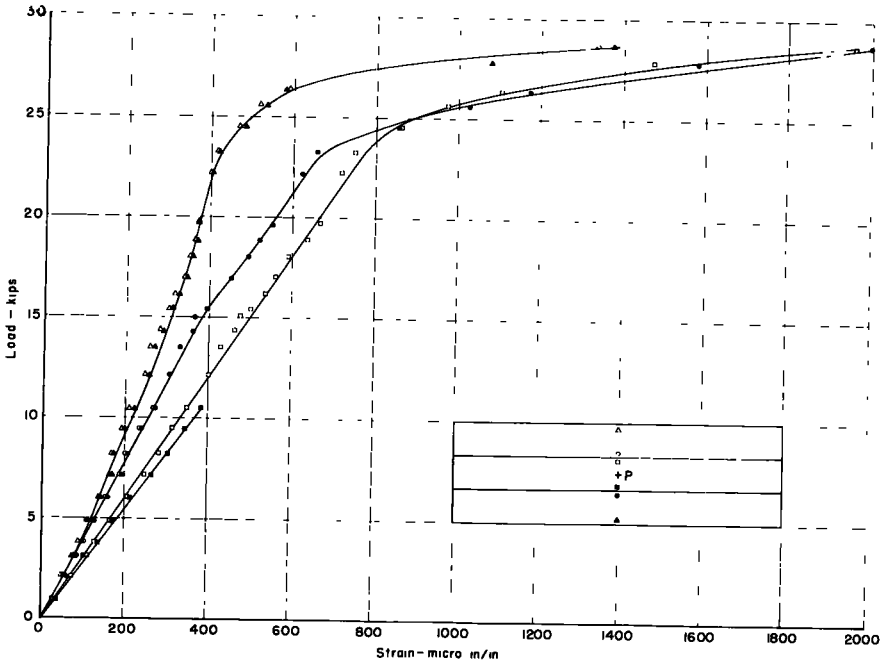

Figure 20. Longitudinal concrete compressive strains—series Ia-Ig.

the outside channels, starting at a load of approximately 15 kips, is apparently due to twisting of these sections. Figure 21 is a plot of the compression-zone depth ratio as a function of load for the center channel section. The depth ratios were computed on the basis of an assumed linear strain distribution between the observed steel strains and the maximum concrete compressive strains in the top fiber of the section. Zone A represents the loads for which the concrete had not cracked and was taking some tension. For the loads in zone B the concrete in the tension zone cracked and hence the value of k was steadily reduced until it reached a constant value in zone C. Zone D is the yield zone. In this zone the total steel stress was essentially constant and the increase in moment capacity was the result of an increase in the internal moment arm. As the yield zone was passed, the depth ratio again began to increase slightly in zone E due to strain hardening of the steel. The minimum observed k-value was found to be in excellent agreement with the value predicted by ultimate strength theory.

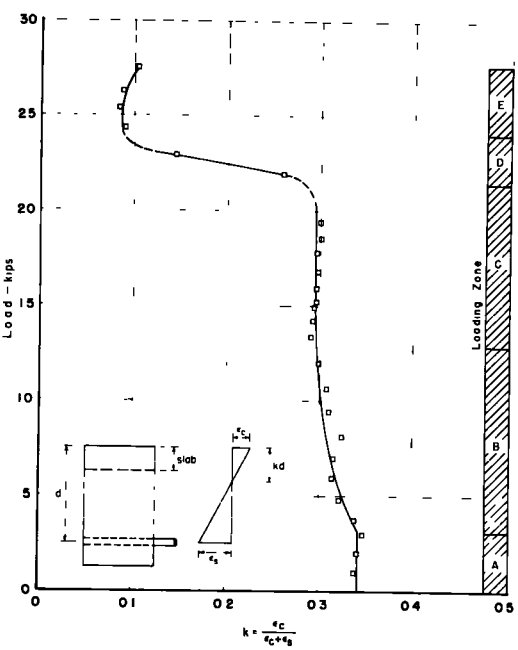

Figure 21. Compression zone depth ratio—series Ia-Ig.

TRANSVERSE STEEL STRAINS

The observed strains in the center - diaphragm reinforcement of the loaded

channel section for loading series Ia-Ie is shown in Figure 22. The significant change in slope at about 11 kips should be noted. This change indicates yielding of the reinforcement and the initiation of load redistribution. It is interesting to note that this load level coincides with the loading at which the corner reaction ceased to increase (Fig. 14). The behavior of the diaphragm was somewhat unexpected in that the observed strains in the tests of the individual sections were relatively small up to loads which resulted in yielding of the longitudinal reinforcement. On the basis of these tests it would appear that load redistribution could be delayed by increasing the diaphragm reinforcement. Assuming an initial yield load of 22 kips for the longitudinal reinforcement, doubling the amount of steel provided in the diaphragms would result in a better balance between longitudinal and transverse reinforcement.

QUALITATIVE RESULTS

Determination of the load reduction coefficient on the basis of ultimate load capacity would be irrelevant for this case because failure in the series Ig test was the result of punching of the slab as shown in Figure 23, whereas the individual sections failed due to excessive yielding of the longitudinal reinforcement followed by a secondary compression failure. The cracking pattern at ultimate load is shown in Figure 24. It should be noted that cracking was confined to the region between intermediate diaphragms at the quarter points. Figure 25 shows the failure of the center diaphragm and the spalling of the slab resulting from the punching failure. This failure occurred at an applied load of 28.7 kips. It is apparent that, even at this load, slip and separation of adjoining channel stems was negligible. After the punching of the center channel, loading was continued by applying load to the outside channels. The final failure due to secondary compression is shown in Figure 26.

SUMMARY AND CONCLUSIONS

The applicable load reduction coefficients (that is, the factors by which the wheel loads should be multiplied to give the reduced equivalent design load for a single section) for the test series discussed are summarized in Table 2. The load reduction coefficients based on yield strains and deflections after load redistribution are slightly more conservative than the coefficients based on working-load strains. This result may have been influenced somewhat by the premature yielding of the diaphragm reinforcement. As has previously been noted, the failure modes at ultimate load were incompatible and therefore ultimate load capacity should not be used as a method of

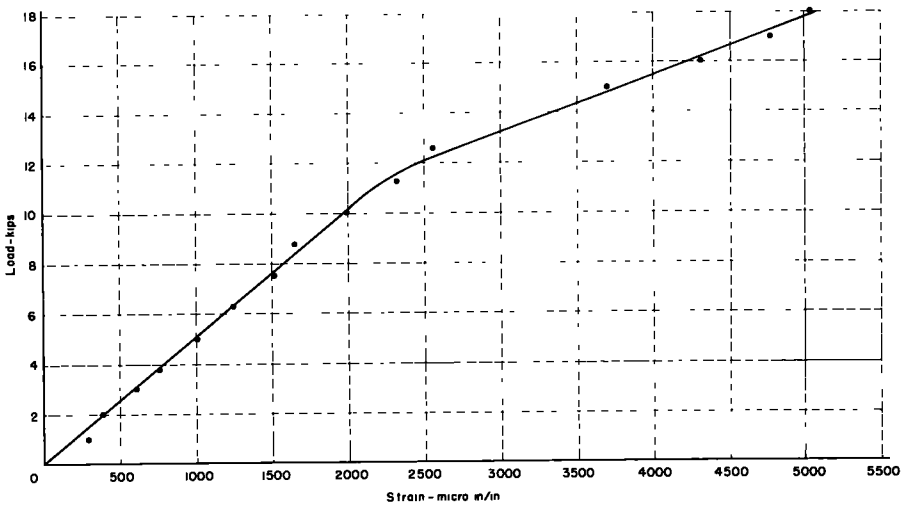

Figure 22. Diaphragm steel strains at midspan.

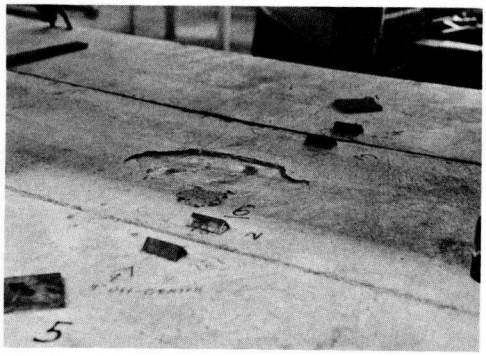

Figure 23. Punching failure.

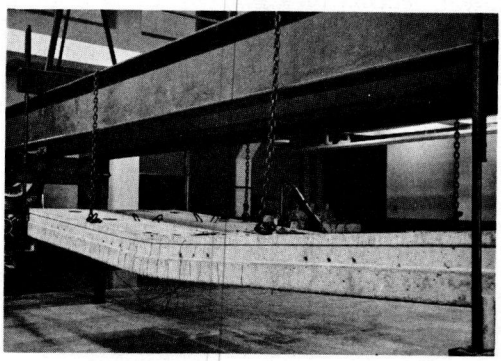

Figure 24. Crack pattern at ultimate load.

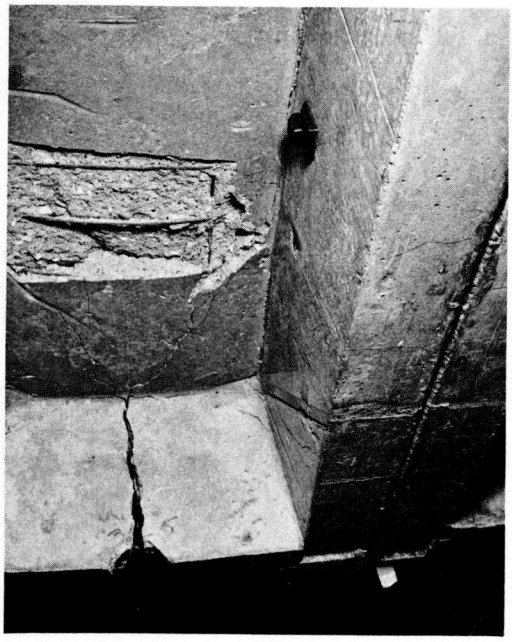

Figure 25. Diaphragm failure.

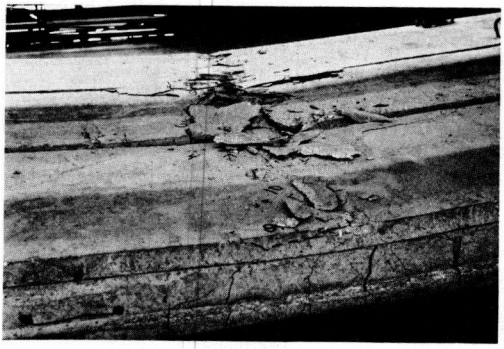

Figure 26. Secondary compression failure.

comparison in this case. Because of the reserve capacity developed by load redistribution, either the equivalent yield-load deflection or the secondary yielding of the principal reinforcement appears to offer the most rational basis for the determination of a suitable load reduction coefficient.

It should be noted that only the principal

TABLE 2

LOAD-REDUCTION COEFFICIENTS

Basis of Determination	Coef.	Comments
Slope of strain curve	0.41	Based on average initial slope (Fig. 18)
Equivalent-yield deflection	0.42	Allowance for load redistribution
Initial-yield strain	0.50	No allowance for load redistribution
Secondary-yield strain	0.42	Allowance for load redistribution
Working-load strain	0.38	
Ultimate load	0.54	Incompatible failure
End reactions	0.37	

test series has been discussed and that the results reported should therefore only be used under conditions which are sufficiently similar to make them applicable. However, the results obtained are believed to be sufficiently encouraging to warrant additional study and experimentation to make more economical designs possible.

ACKNOWLEDGMENTS

The work reported herein was supported by the Missouri State Highway Commission and by the Bureau of Public Roads under a cooperative research agreement. The assistance of Ravi R. Kohli, graduate research assistant, in the performance of the testing and in the reduction of the data is gratefully acknowledged.